Supplementary Information

Atomic-Scale Dynamic Observation Reveals Temperature-Dependent Multistep Nucleation Pathways in Crystallization

Junjie Li[a,b]*, Yunping Li[c], Qiang Li[d], Zhongchang Wang[e], Francis Leonard Deepak[a]*

[a] Nanostructured Materials Group, Department of Advanced Electron Microscopy, Imaging and Spectroscopy, International Iberian Nanotechnology Laboratory (INL), Avenida Mestre Jose Veiga, Braga 4715-330, Portugal

[b] CAS Key Laboratory of Functional Materials and Devices for Special Environments, Xinjiang Technical Institute of Physics & Chemistry, CAS; Xinjiang Key Laboratory of Electronic Information Materials and Devices, 40-1 South Beijing Road, Urumqi 830011, China.

[c] State Key Lab for Powder Metallurgy, Central South University, Changsha 410083, China

[d] School of Mechanical Engineering, University of Shanghai for Science and Technology, Shanghai 200093, China

[e] Department of Quantum and Energy Materials, International Iberian Nanotechnology Laboratory (INL), Avenida Mestre Jose Veiga, 4715-330 Braga, Portugal

*Email: junjie.li@inl.int and leonard.francis@inl.int

Experimental Section

Sample preparation and characterization: A molten salt route was used to prepare the $SrBi_2Ta_2O_9$ (SBTO) nanoplatelets[1]. In a typical synthesis process, the stoichiometric strontium nitrate ($Sr(NO_3)_2$, 99.5%), bismuth oxide (Bi_2O_3, 99.9%) and tantalum oxide (Ta_2O_5, 99.9%) were used as starting materials. 1.1g starting materials were mixed with 1.240 g potassium chloride (KCl, 99.9%) and 0.974 g sodium chloride (NaCl, 99.9%) in an agate mortar for 0.5 h. The mixtures were loaded into an alumina crucible and heated at $850^{o}C$ for 3 h in air, followed by natural cooling to room temperature in a tube furnace. The resultant white samples were washed with deionized water three times to remove the KCl and NaCl solvent, and dried at 60 ℃ for 2 h in an oven. The chemical composition of the obtained products was identified by powder X-ray diffraction (XRD) (X'Pert PRO diffractometer, PANalytical).

In-situ TEM/STEM observation and EDS analysis: The obtained SBTO samples were dispersed in ethanol by ultrasonication for 1 h, and a drop of the white suspension was transferred onto carbon support or heating device. TEM/STEM imaging and EDS mapping were carried out on the Titan Themis TEM equipped with both probe and image Cs corrector and super-X EDS detector at 200 kV, which offered an unprecedented opportunity to probe ultra-small structures with sub-Ångström resolution. The heating experiments were carried out in the TEM using a disposable, micro-electromechanical system (MEMS) device which serves as both support grid for the sample and the heating element by connecting the heating stage to an external power supply[2,3]. The Videos were recorded using Tecnai Imaging and Analysis (TIA) software.

The calculations of electron beam induced temperature rise at different electron doses in TEM.

The electron dose induced maximum temperature rise based on the Bethe theory and Fisher's model[4,5],

$$\Delta T = \frac{I \, \Delta E \, a^2}{4 \, k \, d} \left(1 + 2 \ln \frac{b}{a}\right)$$

where ΔT represents the temperature rise induced by electron beam, I is the beam dose, κ is thermal conductivity, ΔE *is* energy loss of per electron, d is the thickness of sample, b and a represent the radius of conductor and beam radius, respectively. In the thin sample, the electron energy loss is small even for electrons ~200 keV[6]. Here, the energy loss per electron is considered as 6.41×10-16 J, κ =1.0 W/K/m[7-8], d = 20 nm, b = 300 nm. For the electron dose of 25000 e/A^{2}S in Figure 1, the temperature rise ΔT is about 208 K, 187 K and 41 K for Figure 2 and 3. The room temperature is kept at 20 ^{o}C. Therefore, the calculated temperatures (T = ΔT + T_{rm}) of the Bi nanoparticles in Figure 1 to 3 heated by electron beam are about 228 ^{o}C, 207 ^{o}C, and 61 ^{o}C , respectively.

References

1. Y. Li, *et al. Chem. Mater.* **2013**, *25*, 2045-2050.
2. J. Li, Z. Wang, F. L. Deepak, *J. Phys. Chem. Lett.* **2018**, *9*, 961-969.
3. M. A. Asoro, D. Kovar, P. J. Ferreira, *ACS nano* **2013**, *7*, 7844-7852.
4. H.A. Bethe, Handbuch der Physik. vol. 4, 273, Julius Springer (Berilin) (1933).
5. Fisher, S. On the temperature rise in electron irradiated foils. *Radiat. Eff.* **5**, 239-243 (1970).

6. Kim, G.-S. et al. Reduction in thermal conductivity of Bi thin films with high-density ordered nanoscopic pores. *Nanoscale Res. Lett.* **8**, 371 (2013).

7. Song, D. et al. Thermal conductivity of nanoporous bismuth thin films. *Appl. Phys. Lett.* **84**, 1883-1885 (2004).

8. Tachibana, M. Thermal conductivity of Aurivillius compounds Bi_2WO_6, $SrBi_2Ta_2O_9$, and $Bi_4Ti_3O_{12}$. *Solid State Commun.* **211**, 1-3 (2015).

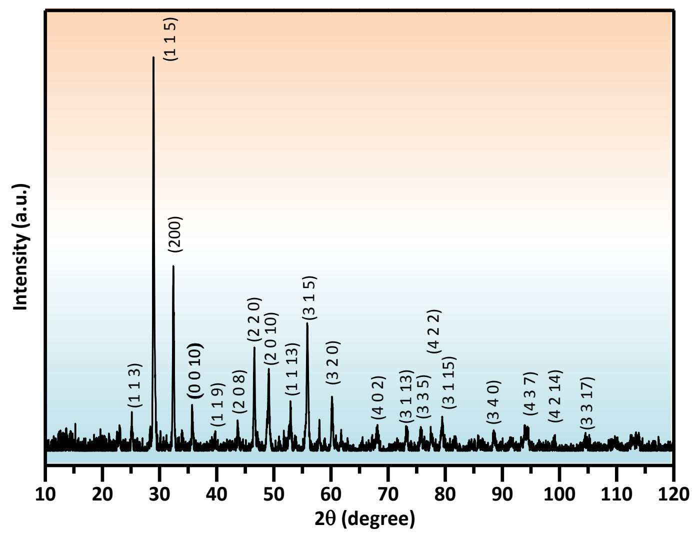

Supplementary Figure 1. XRD analysis. XRD results for the obtained powder samples revealing the successful preparation of pure $SrBi_2Ta_2O_9$ with an orthorhombic structure (JCPDS card no. 05-0519).

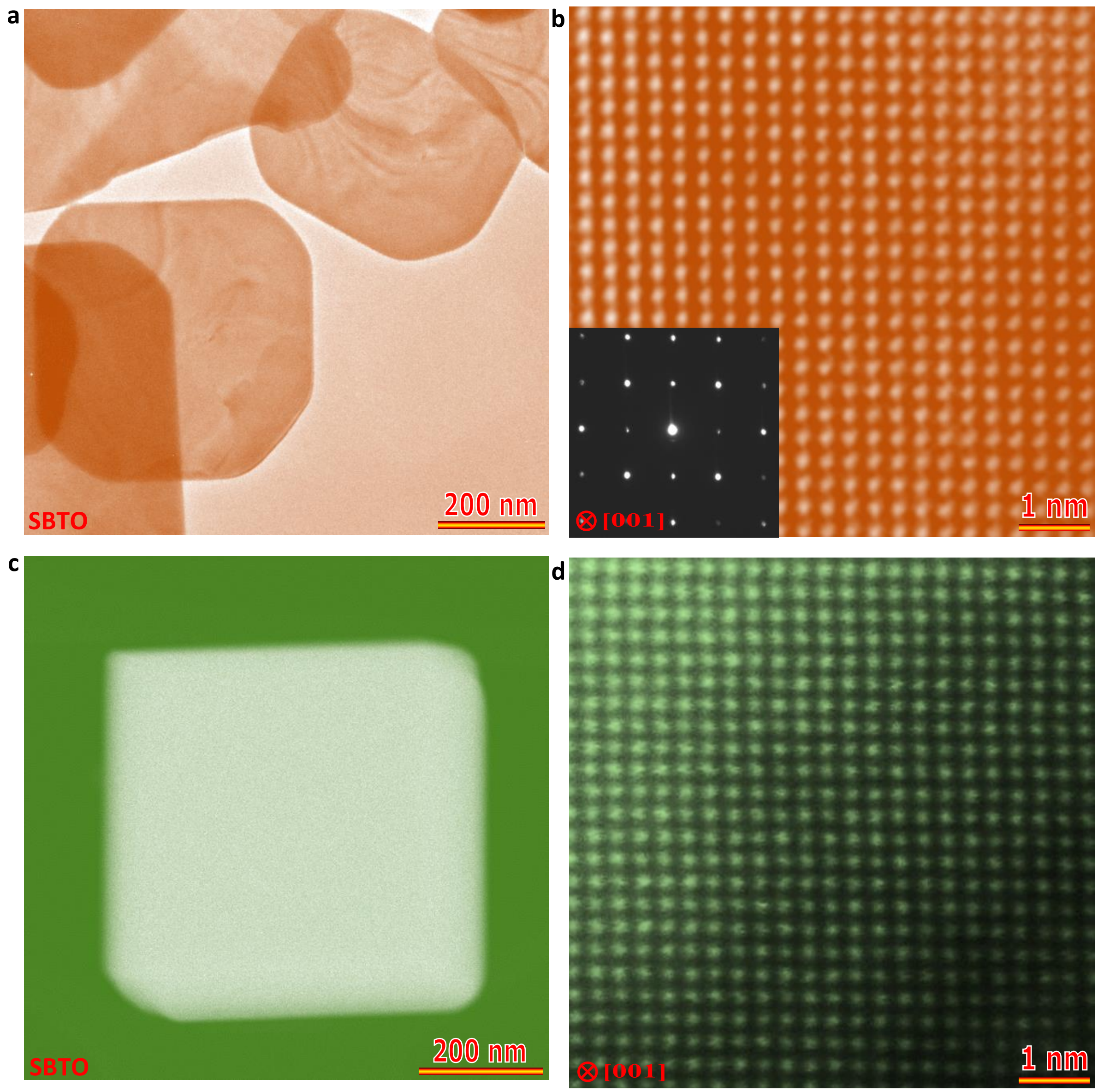

Supplementary Figure 2. Morphology of the sample. a,c, Low magnification TEM (**a**) and HAADF-STEM (**b**) images for the obtained $SrBi_2Ta_2O_9$ product. **b,d,** High resolution TEM and HAADF-STEM images confirming the orthorhombic structure of the $SrBi_2Ta_2O_9$. Inset image in Figure **b** is the diffraction pattern, confirming the single crystal structure.

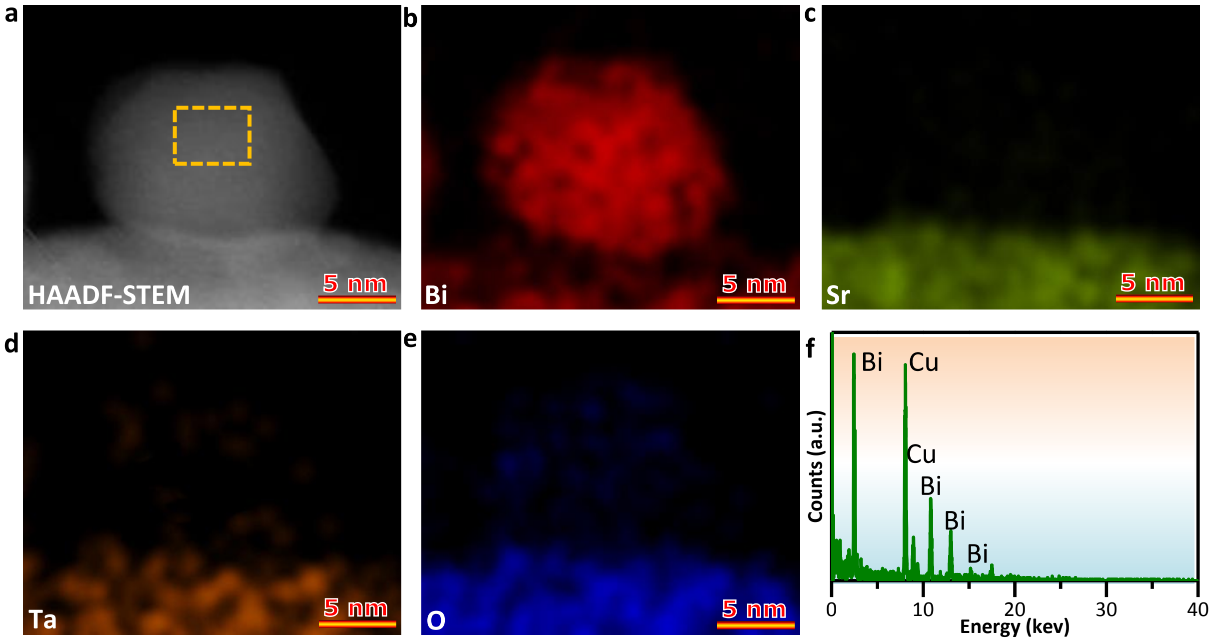

Supplementary Figure 3. Chemical mapping of Bi nanocrystal on SBTO surface. a, HAADF- STEM image. **b–e,** Corresponding energy-dispersive x-ray spectroscopy mapping of Bi (**b**), Sr (**c**), Ta (**d**), and O (**e**). **f,** Corresponding EDS spectrum of the Bi nanocrystal taken in the area marked by an orange square in **a**.

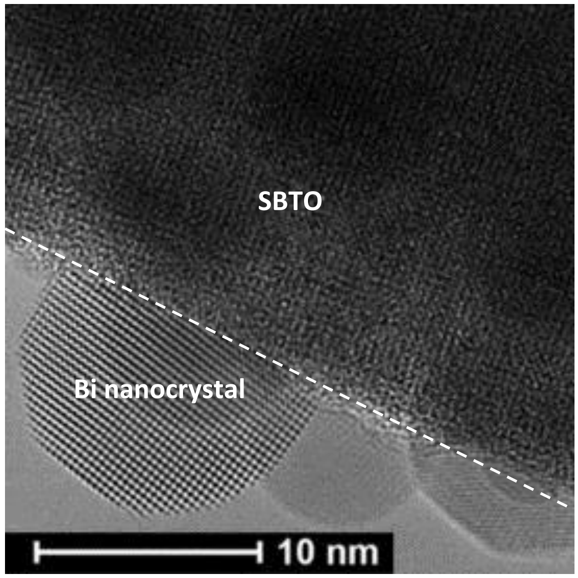

Supplementary Figure 4. Morphology of the segregated Bi nanocrystals. High resolution TEM image showing the formation of the Bi nanocrystals under electron beam irradiation.

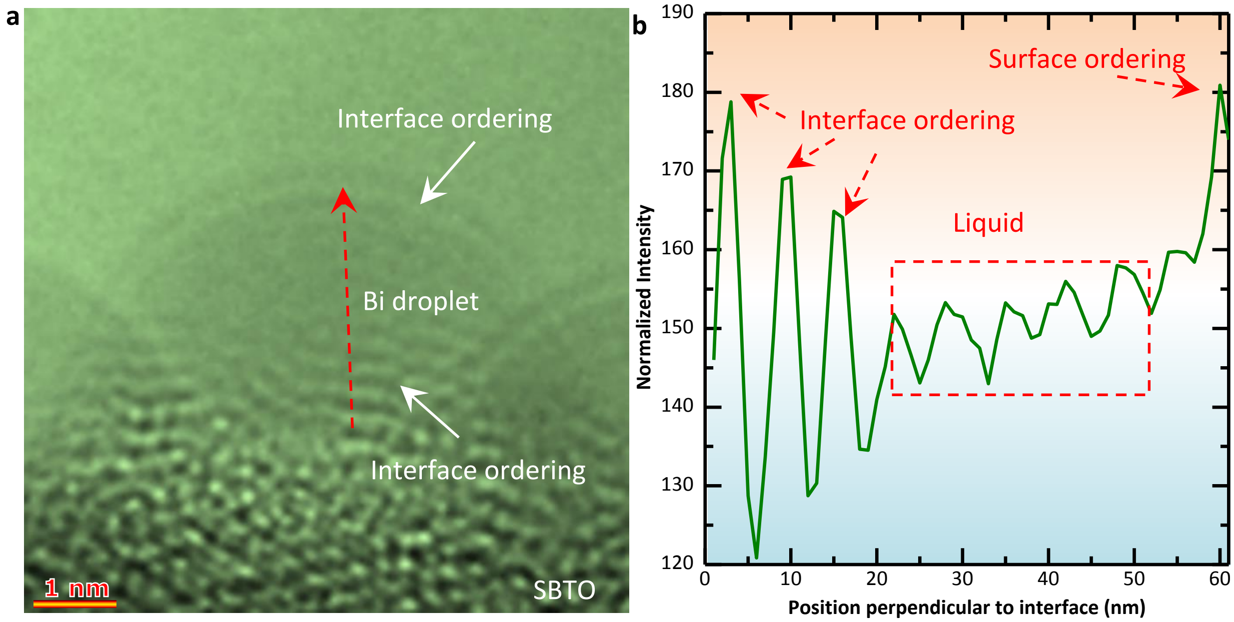

Supplementary Figure 5. Image and line profile for a Bi liquid droplet on $SrBi_2Ta_2O_9$. a, A typical HRTEM image of a Bi droplet on surface of $SrBi_2Ta_2O_9$. b, Line profile showing image intensity along the arrow in (a), illustrating local ordering.

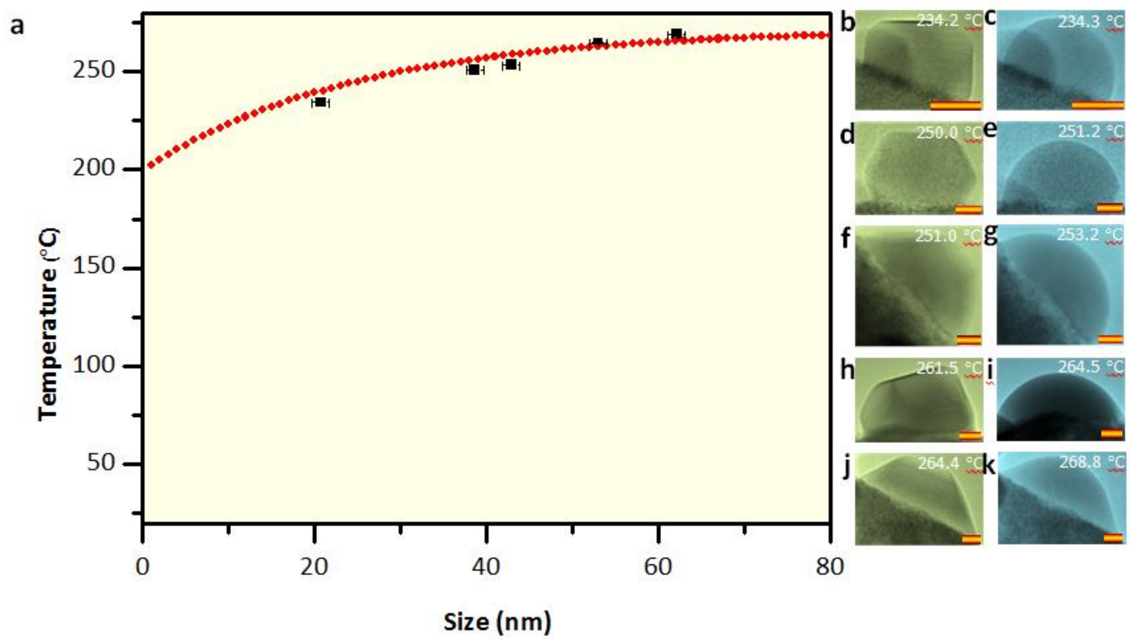

Supplementary Figure 6. Size-dependent melting point of Bi nanocrystal based on the in-situ heating experiment. Error bar is 1nm in Figure S9a, and the scale bar is 10 nm in Figure S9b-k.

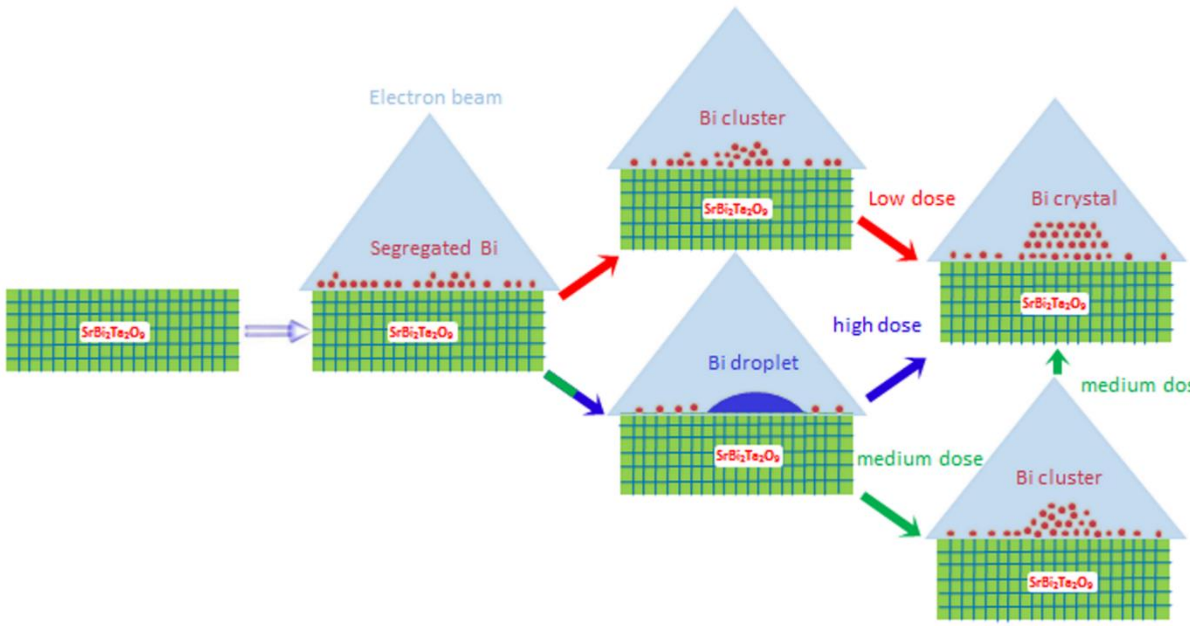

Supplementary Figure 7. Schematic of the electron beam induced Bi nanocrystal growth under different electron dose.

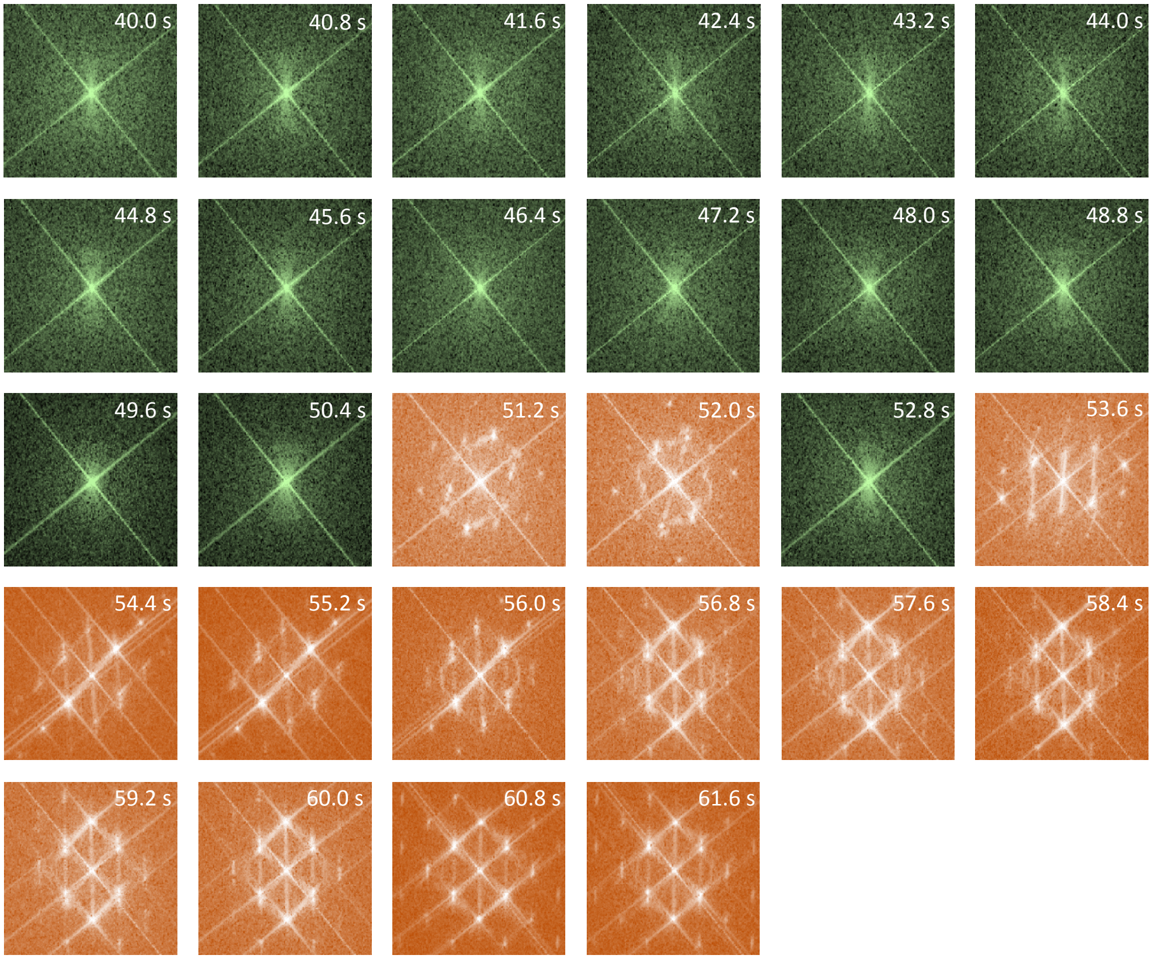

Supplementary Figure 8. Fast Fourier transformation (FFT) analyses. Corresponding FFT analyses during the surface and interface ordering droplet to crystal nucleus two-step nucleation pathway (Video S1). The green and orange colors indicate the liquid and crystal phases, respectively.

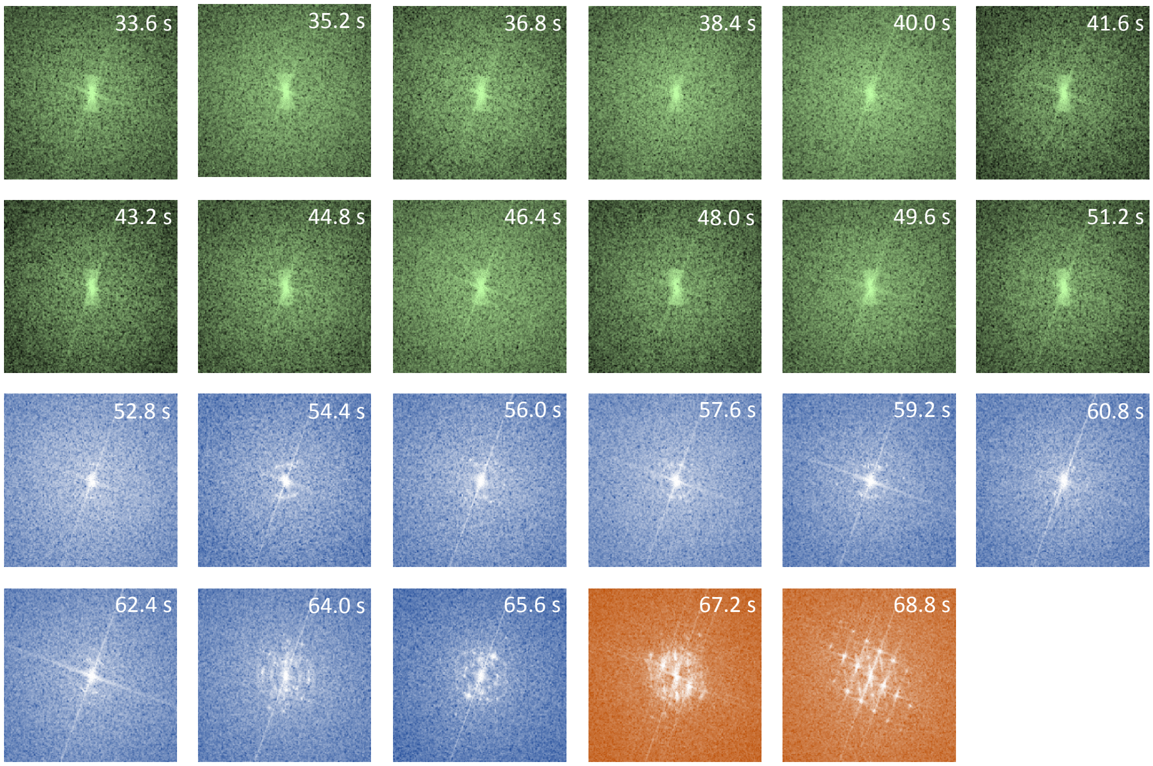

Supplementary Figure 9. Fast Fourier transformation (FFT) analyses. Corresponding FFT analyses during the surface and interface ordered droplet-interior local ordered solid structure-crystal nucleus three-step nucleation pathway (Video S2). The green, blue and orange colors indicate the local ordered solid and crystal phases, respectively.

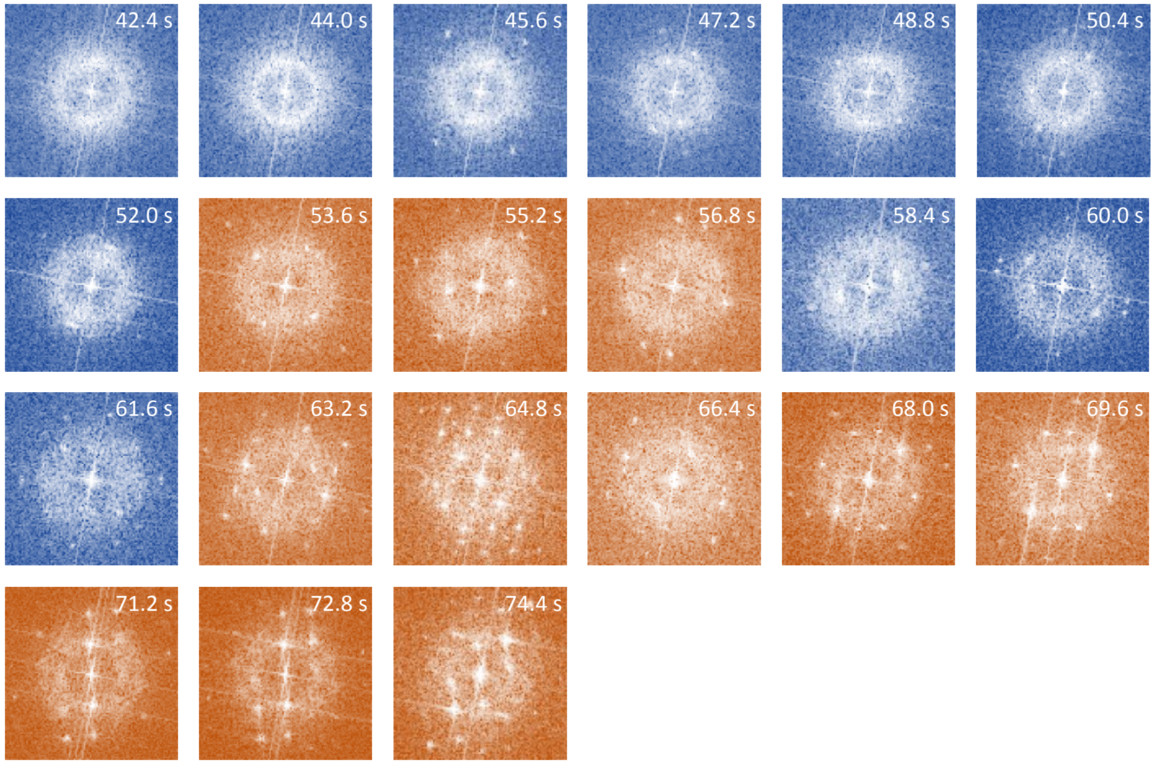

Supplementary Figure 10. Fast Fourier transformation (FFT) analyses. Corresponding FFT analyses during the local ordered cluster structure to crystal nucleus two-step nucleation pathway (Video S3). The blue and orange colors indicate the local ordered cluster and crystal phases, respectively.

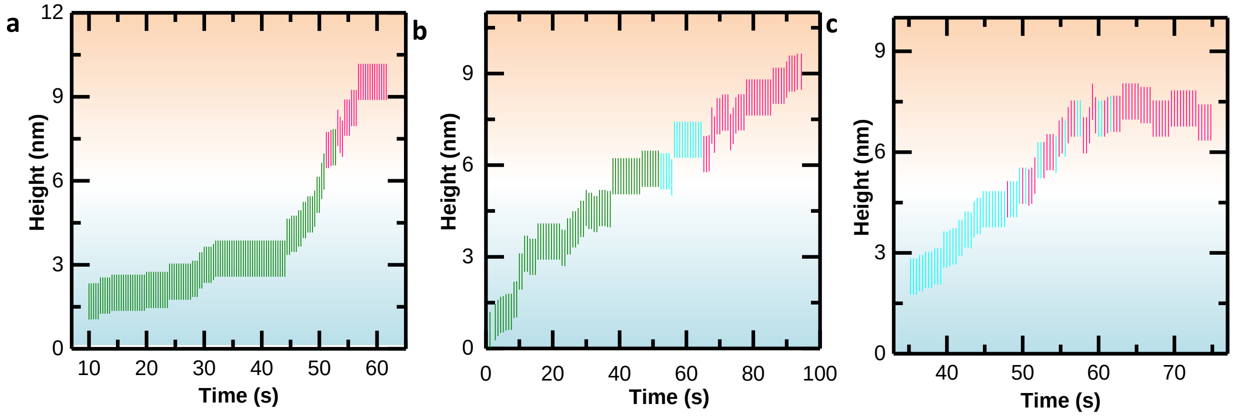

Supplementary Figure 11. Statistical analyses of nucleation dynamics during the multistep nucleation pathways. a-c, Statistical analyses of the height as a function of time (Video S1, S2 and S3). The green, blue and red lines in d-f represent liquid, local ordered solid and crystal phase, respectively.

Video Information

Video S1. Two-step nucleation pathway (surface and interface ordered liquid droplet to crystal nucleus). The Video plays at 2 times the normal speed. The electron dose rate is ~2.5 $\times 10^4$ e/Å^{2}s.

Video S2. Three-step nucleation pathway (surface and interface ordered liquid droplet to interior ordered structure to crystal nucleus). The Video plays at 2 times the normal speed. The electron dose rate is ~1.8 $\times 10^4$ e/Å^{2}s.

Video S3. Two-step nucleation pathway (local ordered cluster structure to crystal nucleus). The Video plays at 2 times the normal speed. The electron dose rate is ~5.0 $\times 10^3$ e/Å^{2}s.